Sulfate formation in sea-salt aerosols: Constraints from oxygen isotopes

B. Alexander,[1] R. J. Park, D. J. Jacob, Q. B. Li,[2] and R. M. Yantosca

Department of Earth and Planetary Sciences and Division of Engineering and Applied Sciences, Harvard University, Cambridge, Massachusetts, USA

J. Savarino,[3] C. C. W. Lee,[4] and M. H. Thiemens

Department of Chemistry and Biochemistry, University of California, San Diego, La Jolla, California, USA

Received 30 November 2004; revised 23 February 2005; accepted 15 March 2005; published 25 May 2005.

[1] We use observations of the mass-independent oxygen isotopic composition ($\Delta^{17}O$) of sulfate in the marine boundary layer (MBL) to quantify the sulfate source from aqueous SO_2 (S(IV)) oxidation by O_3 in alkaline sea-salt aerosols. Oxidation by O_3 imparts a large $\Delta^{17}O$ signature to the resulting sulfate (8.8‰) relative to oxidation by H_2O_2 (0.9‰) or by OH or O_2 (0‰). Ship data from two Indian Ocean Experiment (INDOEX) cruises in the Indian Ocean indicate $\Delta^{17}O$ values usually <1‰ in the submicron sulfate aerosol but considerable variability in the supermicron sulfate with frequent occurrences above 1‰ and up to 6.7‰. The large $\Delta^{17}O$ values are associated with high concentrations of sea-salt aerosols, providing evidence for the S(IV) + O_3 pathway. We use a global chemical transport model (GEOS-CHEM) to interpret quantitatively the INDOEX observations and to assess the global importance of sulfate production in sea-salt aerosols. The model accounts for titration of sea-salt alkalinity in the MBL by uptake of acid gases (SO_2, H_2SO_4, and HNO_3), shutting down the S(IV) + O_3 pathway. We find that this titration occurs rapidly over much of the oceans except at high latitudes (strong sea-salt emission) and is due to both the S(IV) + O_3 reaction and HNO_3 (g) condensation; that is, sulfate formation in sea-salt aerosols is limited by the alkalinity flux from the ocean and by competition for this alkalinity supply from HNO_3 (g). The model is consistent with the $\Delta^{17}O$ magnitudes and patterns in the INDOEX data. Titration of alkalinity is critical for the success of the model simulation. Regeneration of sea-salt aerosol alkalinity by OH uptake is inconsistent with the $\Delta^{17}O$ observations in INDOEX. Model results indicate that sulfate production in sea-salt aerosols decreases MBL SO_2 concentrations and gas phase H_2SO_4 production rates by typically 10–30% (up to >70%) and increases MBL sulfate concentrations by typically >10% (up to 30%). Globally, this mechanism contributes 9% of atmospheric sulfate production and 1% of the sulfate burden. The impact on H_2SO_4 (g) formation and implications for the potential formation of new particles in the MBL warrants inclusion in models examining the radiative effects of sulfate aerosols.

Citation: Alexander, B., R. J. Park, D. J. Jacob, Q. B. Li, R. M. Yantosca, J. Savarino, C. C. W. Lee, and M. H. Thiemens (2005), Sulfate formation in sea-salt aerosols: Constraints from oxygen isotopes, *J. Geophys. Res.*, *110*, D10307, doi:10.1029/2004JD005659.

1. Introduction

[2] Sulfate is a major component of the atmospheric aerosol and drives the formation of new aerosol particles through nucleation. The implications for scattering of solar radiation and for cloud microphysics represent one of the largest uncertainties in current assessments of climate change [*Intergovernmental Panel on Climate Change* (*IPCC*), 2001]. Sulfate is mainly produced within the atmosphere by oxidation of SO_2, which is itself directly emitted (fossil fuel combustion, industrial processes, and volcanoes) or produced within the atmosphere by oxidation of reduced sulfur species such as dimethyl sulfide (DMS) emitted by oceanic phytoplankton. The oxidation of SO_2 can take place in the gas phase [*Stockwell and Calvert*, 1983] and in the aqueous phase [*Schwartz*, 1987]. The branching ratio between these two pathways is not well

[1]Now at Department of Atmospheric Sciences, University of Washington, Seattle, Washington, USA.

[2]Now at Jet Propulsion Laboratory, Pasadena, California, USA.

[3]Now at Laboratoire de Glaciologie et Géophysique de l'Environnement/CNRS, St Martin d'Hères, France.

[4]Now at URS Corporation, Santa Ana, California, USA.

0148-0227/05/2004JD005659$09.00

understood but plays a critical role in determining the nucleation potential and optical properties of the sulfate aerosol.

[3] Oxidation in the aqueous phase is thought to occur primarily in clouds because of their high liquid water content [*Schwartz*, 1987]. However, deliquescent sea-salt and dust aerosols have also been suggested as important sites for aqueous phase sulfate production [*Chameides and Stelson*, 1992; *Sievering et al.*, 1991; *Song and Carmichael*, 2001] because of the rapid rate of SO_2 oxidation by ozone in alkaline solutions. Production in sea-salt aerosols could greatly affect sulfate concentrations and size distributions in the marine boundary layer (MBL) [*Song and Carmichael*, 2001], with consequences for both direct radiative forcing [*Shaw*, 1983] and indirect radiative forcing via cloud formation [*Charlson et al.*, 1987]. Here we exploit oxygen isotope measurements of sulfate in the MBL to quantify production in sea-salt aerosols, and we interpret the results in terms of sources and titration of MBL alkalinity.

[4] Gas phase oxidation of SO_2,

$$\begin{aligned} &SO_2 + OH + M \rightarrow HOSO_2 + M, \\ (R1) \qquad &HOSO_2 + O_2 \rightarrow HO_2 + SO_3, \\ &SO_3 + H_2O + M \rightarrow H_2SO_4 + M, \end{aligned}$$

produces H_2SO_4 (g) that can nucleate new particles under favorable conditions, increasing aerosol number density and the population of cloud condensation nuclei (CCN) [*Andronache et al.*, 1997; *Kumala et al.*, 2000; *Weber et al.*, 2001]. Sulfate produced in the aqueous phase is present in larger particles and does not lead to nucleation of new particles. Aqueous phase sulfate formation involves dissolution of SO_2 followed by acid-base dissociation of $SO_2 \cdot H_2O$ to HSO_3^- ($pK_{a1} = 1.9$) and SO_3^{2-} ($pK_{a2} = 7.2$). We refer to total dissolved SO_2 as $S(IV) \equiv SO_2 \cdot H_2O + HSO_3^- + SO_3^{2-}$. Oxidation of S(IV) takes place by dissolved H_2O_2,

$$(R2a) \qquad HSO_3^- + H_2O_2 \leftrightarrow SO_2OOH^- + H_2O$$

$$(R2b) \qquad SO_2OOH + H^+ \rightarrow H_2SO_4,$$

and dissolved O_3,

$$(R3) \qquad O_3 + SO_3^{2-} \rightarrow O_2 + SO_4^{2-}.$$

The rate of (R3) is dependent on the partitioning of S(IV) as SO_3^{2-} and is significant only at pH > 6 [*Chameides*, 1984; *Calvert et al.*, 1985]. In contrast, the rate of (R2) is independent of pH [*McArdle and Hoffmann*, 1983]. S(IV) can also be oxidized in the aqueous phase by other oxidants, including O_2 catalyzed by Fe(III) and Mn(II) [*Jacob and Hoffmann*, 1983], NO_2 [*Lee and Schwartz*, 1983], NO_3 [*Feingold et al.*, 2002], and HNO_4 [*Warneck*, 1999; *Dentener et al.*, 2002]. These other oxidants are thought to be of little importance on a global scale, although they may be significant regionally. HOCl and HOBr have been proposed as potentially important S(IV) oxidants in the MBL [*Vogt et al.*, 1996; *von Glasow et al.*, 2002; *von Glasow and Crutzen*, 2004], but there is so far no observational evidence.

[5] Global models simulating sulfur chemistry generally consider the aqueous phase production of sulfate to proceed in clouds only [*Chin et al.*, 1996; *Kasibhatla et al.*, 1997; *Koch et al.*, 1999; *Barth et al.*, 2000; *Tie et al.*, 2001; *Liao et al.*, 2003]. Some models omit the O_3 oxidation pathway [*Chin et al.*, 1996; *Kasibhatla et al.*, 1997; *Koch et al.*, 1999] since H_2O_2 is the dominant oxidant under typical bulk cloud pH conditions (pH < 5) [*Jacob*, 2000]. However, if the pH $\approx$ 8 of surface seawater applies to sea-salt aerosols, then the S(IV) loss rate constant for oxidation by O_3 in these aerosols would be 10^5 times faster than in-cloud oxidation by H_2O_2, more than making up for their lower liquid water content [*Chameides and Stelson*, 1992]. Because of the high CO_3^{2-}/HCO_3^- content of seawater, sea-salt aerosols have a high acid-buffering capacity or alkalinity, equal to 0.07 equivalents per kilogram (eq kg^{-1}) of dry sea-salt emitted [*Gurciullo et al.*, 1999]. The range of global estimates for the sea-salt flux to the atmosphere, 5000–10,000 Tg yr^{-1} [*Chin et al.*, 2002; *Gong et al.*, 2002; *Grini et al.*, 2002], thus implies a source of alkalinity of 0.35–0.7 T eq yr^{-1}, enabling the fast oxidation of 6.1–12.2 Tg S yr^{-1} to sulfate under high-pH conditions. Comparing this to the global oceanic DMS emission of 11–25 Tg S yr^{-1} [*Chin et al.*, 1996; *Koch et al.*, 1999; *IPCC*, 2001] highlights the potential importance of this pathway.

[6] The alkalinity budget of the MBL is thus critical for quantifying the importance of S(IV) oxidation in sea-salt particles. Once the alkalinity is consumed, the pH of the aerosols drops rapidly, and (R3) effectively shuts off [*Chameides and Stelson*, 1992]. A schematic for the processes involved is shown in Figure 1. Alkalinity supplied by the emitted sea salt is consumed not only by (R3) but also by condensation of gas phase acids (H_2SO_4, HNO_3, and RCOOH) [*Davies and Cox*, 1998; *Ten Brink*, 1998; *Katoshevski et al.*, 1999; *Song and Carmichael*, 1999; *Guimbaud et al.*, 2002]. Coagulation of acid sulfate particles would also consume sea-salt aerosol alkalinity, but it is negligibly slow relative to condensation of acid gases [*Gong and Barrie*, 2003]. Ammonia emitted from the ocean and subsiding from the free troposphere is an additional source of alkalinity to the MBL; however, it is not significantly taken up by droplets with pH > 6 [*Jacob et al.*, 1986] and therefore cannot sustain sea-salt aerosol alkalinity to allow (R3) to proceed.

[7] Alkalinity sources in excess of bulk seawater alkalinity have been proposed to impact the sulfur cycle in the MBL. Sea-salt aerosol measurements of excess calcium are attributed to a biogenic source of alkalinity ($CaCO_3$ produced by coccolithophore phytoplankton), which would increase the estimated alkalinity flux from the ocean surface, particularly in regions of high oceanic productivity [*Sievering et al.*, 2004]. On the basis of laboratory experiments, *Laskin et al.* [2003] suggested that the reaction of the hydroxyl radical (OH) with deliquesced NaCl particles could continuously supply alkalinity through OH^- formation at a rate comparable to sulfate formation via (R3). However, the atmospheric implications of Laskin et al.'s results have been challenged because of their neglect of gas phase diffusion limitation for OH uptake [*Sander et al.*, 2004] and acidification by acids other than SO_2 [*Keene and*

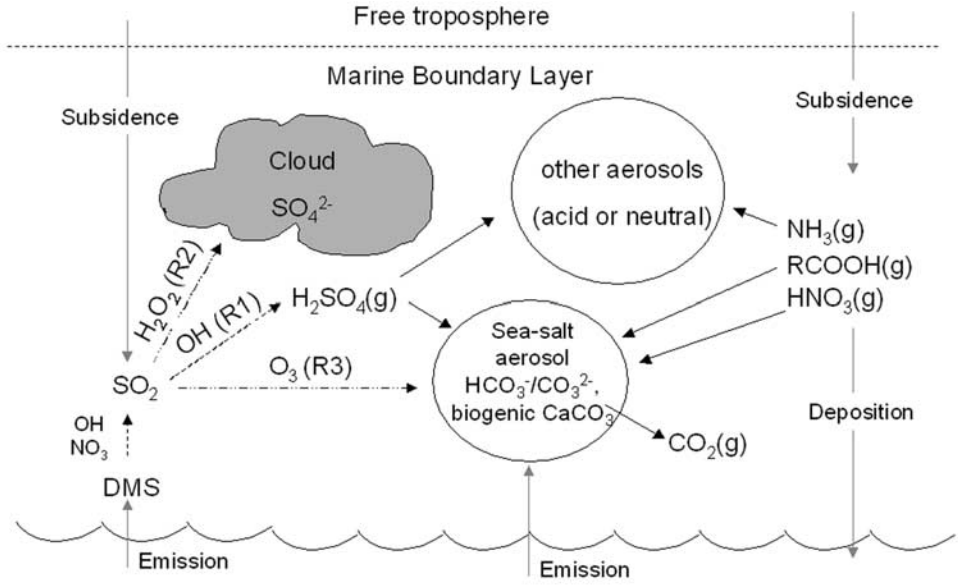

Figure 1. Processes determining sea-salt aerosol alkalinity in the marine boundary layer. Dashed lines indicate gas phase oxidation, dash-dotted lines indicate aqueous phase oxidation, and solid lines indicate gas-aerosol transfer. Shaded lines indicate emissions, subsidence from the free troposphere, and deposition to the surface. Sea-salt aerosol alkalinity emitted to the atmosphere is consumed by uptake of SO_2, H_2SO_4, HNO_3, and organic acids (RCOOH). Ammonia subsiding from the free troposphere or emitted by the ocean does not condense on sea-salt aerosols (see text) and thus does not replenish the consumed alkalinity.

Pszenny, 2004]. As we will see, the observed oxygen isotopic composition of sulfate argues against a continuous supply of alkalinity from the NaCl + OH reaction.

[8] We use here ship measurements of the oxygen isotopic composition of sulfate over the Indian Ocean from the Indian Ocean Experiment (INDOEX) campaign [*Ramanathan et al.*, 2001] to gain information on sulfate formation pathways in the MBL. The different oxidants (O_3, H_2O_2, and OH) have distinct oxygen isotopic compositions that are passed to sulfate upon oxidation [*Savarino et al.*, 2000]. Constraints from oxygen isotopes have been used previously to infer the formation pathways of sulfate in continental air [*Lee et al.*, 2001; *Lee and Thiemens*, 2001] and in ice cores [*Alexander et al.*, 2002, 2004]. However, quantitative interpretation is difficult on the basis of measurements alone. We show here that a global model simulation including oxygen isotopes can help for that purpose and can also allow for extrapolation to the global scale.

2. Isotopic Constraints on Sulfur Oxidation Pathways

[9] Kinetic and equilibrium processes such as isotopic exchange or diffusion fractionate oxygen isotopes according to the following relation [*Matsuhisa et al.*, 1978]:

$$\frac{R^{17}}{R_0^{17}} = \left(\frac{R^{18}}{R_0^{18}}\right)^{0.52}, \qquad (1)$$

where $R^x = [^x\mathrm{O}]/[^{16}\mathrm{O}]$ is the isotopic ratio (x = 17 or 18), measured relative to an international reference standard (R_0^x). The standard used for oxygen is standard mean ocean water. The relationship (1) is termed mass-dependent fractionation. Any process that does not follow (1) is termed mass-independent and is characterized by the $\Delta^{17}O$ value where [*Farquhar et al.*, 2000]

$$\Delta^{17}\mathrm{O}(‰) = 10^3 \times \left[\left(\frac{R^{17}}{R_0^{17}}\right) - \left(\frac{R^{18}}{R_0^{18}}\right)^{0.52}\right]. \qquad (2)$$

For mass-dependent fractionation, $\Delta^{17}O$ = 0‰. Atmospheric H_2O and O_2 have $\Delta^{17}O$ at or near 0‰ [*Thiemens*, 1999]. SO_2 has $\Delta^{17}O$ = 0‰ throughout the troposphere because of isotopic exchange with water vapor [*Holt et al.*, 1981], which erases any source-derived isotopic signature.

[10] Both atmospheric O_3 and H_2O_2 have positive $\Delta^{17}O$ values. Photochemical model calculations by *Lyons* [2001] constrained with laboratory data [*Morton et al.*, 1990; *Thiemens and Jackson*, 1990; *Janssen et al.*, 1999; *Mauersberger et al.*, 1999] indicate $\Delta^{17}O$ = 35‰ for surface O_3, increasing to 38‰ at the tropopause. These values are at the upper end of tropospheric measurements, which, however, are likely to be biased low because of sampling artifacts [*Brenninkmeijer et al.*, 2003]. H_2O_2 measurements from rainwater in La Jolla, California, show a range of 1.3–2.2‰ [*Savarino and Thiemens*, 1999] with an average of 1.7‰. The photochemical model calculations by *Lyons* [2001] indicate $\Delta^{17}O$ = 0.9–1.8‰ for tropospheric HO_2, the precursor of H_2O_2, which is consistent with the H_2O_2 measurements. In contrast, OH has $\Delta^{17}O$ = 0‰ because of isotopic exchange with water vapor [*Dubey et al.*, 1997; *Lyons*, 2001].

[11] Laboratory experiments show that a positive $\Delta^{17}O$ in sulfate originates from aqueous phase oxidation of SO_2 by

H_2O_2 and O_3 through simple transfer of the isotopic anomaly from the oxidant to the sulfate product following (R2) [*Savarino et al.*, 2000],

$$HSO_3^- + H_2O_2 \rightarrow \Delta^{17}O_{SO_4^{2-}} = 0.9‰,$$

and following (R3),

$$SO_3^{2-} + O_3 \rightarrow \Delta^{17}O_{SO_4^{2-}} = 8.8‰.$$

Other sulfate sources including gas phase oxidation by OH in the troposphere, metal-catalyzed oxidation by O_2, and primary sulfate are mass-dependently fractionated ($\Delta^{17}O = 0$) [*Savarino et al.*, 2000; *Lee et al.*, 2002]. Since S(IV) oxidation by O_3 (R3) is the only mechanism producing sulfate $\Delta^{17}O$ values >1‰, observations of atmospheric sulfate $\Delta^{17}O$ values >1‰ are a robust indicator of the importance of O_3 in sulfate formation. Sulfate in the atmosphere does not undergo further isotopic exchange.

[12] The $\Delta^{17}O$ values of sulfate formed in fresh sea-salt aerosols should be determined by O_3 oxidation and should have $\Delta^{17}O = 8.8‰$, while $\Delta^{17}O$ values of sulfate formed in clouds should be <1‰ because of low cloud water pH. Rainwater pH during the two INDOEX cruises discussed in this work ranged between 3.7 and 5.6 [*Kulshrestha et al.*, 1999], sufficiently low to suppress S(IV) oxidation by O_3. $\Delta^{17}O$ measurements for MBL sulfate thus provide a means to distinguish between S(IV) oxidation in sea-salt aerosols versus other processes.

3. Ship Cruise Data

[13] A high-volume air sampler with a four-stage cascade impactor was operated on board the scientific vessel OR/V *Sagar Kanya* during its 120th cruise (cruise 120) from 27 December 1996 to 31 January 1997 as part of the pre-INDOEX 1997 campaign and during cruise 133 from 18 February to 31 March 1998 as part of the INDOEX 1998 first field phase. The high-volume air sampler was installed in the front of the ship to minimize contamination from the ship exhaust. Cruise tracks are shown in Figure 2. They covered the Indian Ocean from about 15°N to 15°S latitude and from 60° to 79°E longitude. Glass filter samples were collected over 48-hour intervals. Immediately after collection, the filters were placed inside a sealed plastic bag and were refrigerated. A total of 14 collections were made during pre-INDOEX 1997, and 12 collections were made during INDOEX 1998, covering the course of each cruise. After each cruise the filters were sent to La Jolla, California, for isotopic analysis.

[14] The collected sulfate was divided into two groups according to particle size: fine ($\leq$1 μm) and coarse (>1 μm). The filters were submerged in a beaker with 100 mL of Millipore water and were placed in an ultrasonic bath for 15 min to dissolve sulfate ions. Any insoluble matter was filtered from the solution with 0.22 μm pore size cellulose filters. Activated carbon was added to the solution and was filtered to eliminate dissolved organic species.

[15] For the pre-INDOEX 1997 samples, sulfate was extracted from solution through precipitation as barite ($BaSO_4$) using $BaCl_2$, followed by conversion of $BaSO_4$ to CO_2 and fluorination (BrF_5) of CO_2 to yield O_2 suitable for oxygen isotopic analysis as described by *Bhattacharya and Thiemens* [1989]. The precision of these $\Delta^{17}O$ measurements is ±0.1‰. For the INDOEX 1998 samples we used a more recently developed technique [*Savarino et al.*, 2001; *Alexander et al.*, 2002]. Briefly, the sulfate ions were separated by ion chromatography, were converted to Ag_2SO_4 using a cation exchange column, and were pyrolyzed at 1000°C in a continuous flow system to yield O_2 suitable for oxygen isotopic analysis. The precision of the $\Delta^{17}O$ measurements with this method is ±0.3‰.

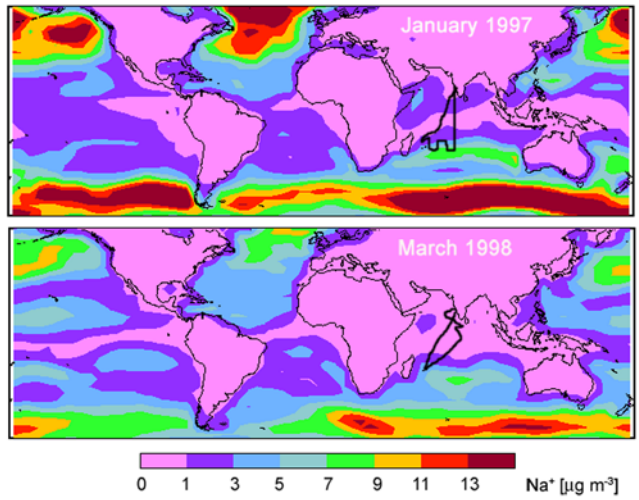

Figure 2. Simulated monthly mean sea-salt Na^+ concentrations (μg m^{-3}) in January 1997 and March 1998 averaged over the 0–100 m altitude column. Cruise tracks for the 1997 pre–Indian Ocean Experiment (INDOEX) cruise and the 1998 INDOEX cruise are shown as thick lines.

[16] The isotopic compositions reported in this paper have been corrected for primary sea-salt sulfate ($ssSO_4^{2-}$) using Na^+ concentration measurements, according to the relation $([ssSO_4^{2-}]/[Na^+])_{sample} = ([SO_4^{2-}]/[Na^+])_{seawater} = 0.252$ mol mol^{-1} [*Calhoun et al.*, 1991]. Subtraction of $ssSO_4^{2-}$ from the sulfate measurements yields non-sea-salt sulfate ($nssSO_4^{2-}$). For the INDOEX 1998 cruise, $[Na^+]$ was measured directly in our samples by ion chromatography (Dionex 4500). For the pre-INDOEX 1997 cruise we used $[Na^+]$ data from a bulk aerosol sampler (D. L. Savoie, personal communication, 2004) running continuously next to our sampler, and we assumed a 10/90 fine/coarse mass fraction for sea-salt aerosols [*Gong et al.*, 2002].

[17] Figure 3 shows the $nssSO_4^{2-}$ $\Delta^{17}O$ (‰) and Na^+ concentration (μg m^{-3}) measurements plotted against latitude. The pre-INDOEX 1997 $\Delta^{17}O$ values are <1‰ except for the coarse $nssSO_4^{2-}$ south of the equator which displays large values, up to 6.7‰. A similar latitudinal gradient is observed for $[Na^+]$. During the INDOEX 1998 cruise, $\Delta^{17}O$ was generally <1‰ except for two samples, both collected south of the equator. There is thus evidence of S(IV) + O_3 as an important source of sulfate under some conditions but not in others. Association with high Na^+ concentrations

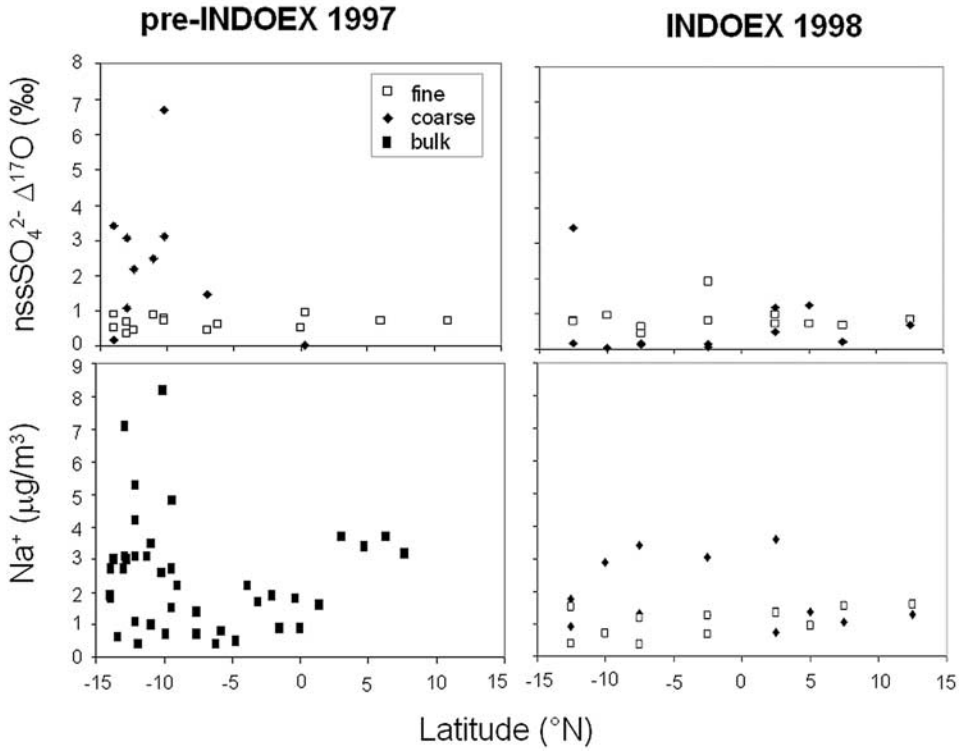

Figure 3. Measurements of (top) non-sea-salt sulfate ($nssSO_4^{2-}$) $\Delta^{17}O$ and (bottom) Na^+ concentrations for pre-INDOEX 1997 and INDOEX 1998. The data are segregated as fine (<1 μm diameter, open squares) and coarse (>1 μm diameter, solid diamonds) aerosols for all but Na^+ for the 1997 pre-INDOEX cruise. Solid squares are bulk aerosol measurements from D. L. Savoie (personal communication, 2004).

(>4 μg m^{-3}) is consistent with this source taking place in sea-salt aerosols.

4. GEOS-CHEM Model

[18] We use the GEOS-CHEM global three-dimensional (3-D) model of coupled aerosol-oxidant chemistry [*Park et al.*, 2004] to simulate the $\Delta^{17}O$ observations from the two cruises. The model (version 5.04) (available at http://www-as.harvard.edu/chemistry/trop/geos/geos_versions.html) uses assimilated meteorological data from the NASA Goddard Earth Observing System (GEOS) including winds, convective mass fluxes, mixed layer depths, temperature, precipitation, and surface properties. Meteorological data have 6-hour temporal resolution (3-hour for surface variables and mixing depths). Meteorological fields for 1996–1997 have a horizontal resolution of 2° latitude by 2.5° longitude (2° × 2.5°) with 46 sigma vertical levels (including 3 below 1 km for a column based at sea level). Meteorological fields for 1998 have 1° × 1° horizontal resolution with 48 sigma vertical levels (including 7 below 1 km for a column based at sea level). For input into GEOS-CHEM we degrade the horizontal resolution to 4° × 5°. We conduct two simulations, one for July 1996 to June 1997 and one for January to April 1998.

[19] The sulfur simulation is as described by *Park et al.* [2004] with the addition of ship emissions of SO_2 from the ship emissions assessment inventory [*Corbett et al.*, 1999], sea-salt emissions from the surface ocean (two size classes partitioned at a radius of 1 μm), and sulfate formation through S(IV) + O_3 in sea-salt aerosols. Sulfate produced by each oxidation pathway is transported as a separate "tracer" in the model with a corresponding $\Delta^{17}O$ value. Total sulfate and $\Delta^{17}O$ are determined locally by addition.

[20] Anthropogenic sources of sulfur in the model total 67.5 Tg S yr^{-1}, including 4.2 Tg S yr^{-1} from ships. This anthropogenic sulfur is emitted as SO_2 except for 3% as primary SO_4^{2-} (5% in Europe) [*Chin et al.*, 2000]. Natural sources include oceanic phytoplankton (12.4 Tg S yr^{-1} as DMS), volcanoes (5.5 Tg S yr^{-1} as SO_2), and biomass burning (1.3 Tg S yr^{-1} as SO_2). The emission flux of sea-salt (particle m^{-2} s^{-1}) is calculated as a function of dry particle size and local 10 m wind speed following the empirical relationship of *Monahan et al.* [1986] and is integrated over fine (0.1–1 μm) and coarse (1–10 μm) size ranges. All emissions are distributed vertically by mass in the local mixed layer.

[21] The simulation includes 10 chemical species transported in the model: DMS, SO_2, sulfate (as six separate tracers), methanesulfonic acid, NH_3, NH_4^+, NO_3^-, H_2O_2, submicron sea salt, and supermicron sea salt. Sulfate formation from oxidation of SO_2 takes place by gas phase oxidation by OH and by in-cloud oxidation by H_2O_2 and O_3. A cloud pH of 4.5 is assumed for the latter. The oxidation of S(IV) by O_3 in sea-salt aerosols is described in section 5. We use monthly mean oxidant (OH, O_3, and NO_3) concentration fields, H_2O_2 production rates and photolysis frequencies, and total inorganic nitrate (HNO_3 (g) plus aerosol NO_3^-) concentrations from a coupled aerosol-oxidant simulation as described by *Park et al.* [2004].

[22] Wet deposition of aerosols is as described by *Liu et al.* [2001] and includes contributions from scavenging in

Table 1. Global Sea-Salt Aerosol Budgets Reported in the Literature[a]

	Emission, Tg yr^{-1}	Size Range Considered,[b] μm	Dry Deposition[c]	Wet Deposition[c]	Lifetime, hours			Burden, Tg
					$r < 1$ μm	$r > 1$ μm	Total	
This work	5,370	0.1–10	60%	40%	31	8	9.6	5.9
Liao et al. [2004]	6,060	0.031–64	NA	NA	NA	NA	9.6	6.9
Gong et al. [2002]	10,100	0.2–20.5	93%	7%	80–360	0.3–10	NA	NA
Chin et al. [2002]	5,810–7,560	0.1–10	99%	1%	NA	NA	NA	8–14
Grini et al. [2002]	6,500	0.03–16.4	66%	34%	NA	NA	NA	6.1
Takemura et al. [2000]	3,530	0.1–10	46%	54%	NA	NA	19.2	5.6
Tegen et al. [1997]	5,900	2–16	NA	NA	NA	NA	NA	11.4

[a]NA, not available.
[b]Dry particle radius r.
[c]As percentages of total deposition, which balances emission.

convective updrafts, rain out and washout from convective anvils and large-scale precipitation, and return to the atmosphere following reevaporation. Dry deposition velocities for sea-salt aerosols (and sulfate formed in sea-salt aerosols) are computed with the size-dependent scheme of *Zhang et al.* [2001] integrated over each model size bin and accounting for hygroscopic growth as a function of relative humidity [*Gerber*, 1985]. Dry deposition velocities for all other species are computed with a standard resistance-in-series scheme based on *Wesely* [1989] as described by *Wang et al.* [1998].

[23] Our global sea-salt aerosol budget is given in Table 1, and global maps of surface (0–100 m altitude) air concentrations for January 1997 (pre-INDOEX 1997) and March 1998 (INDOEX 1998) are shown in Figure 2. Our sea-salt emission (5370 Tg yr^{-1}) and burden (5.9 Tg) are within the range reported in the literature (Table 1). Differences between models reflect, in part, the accounting of different size ranges. Our simulated monthly average sea-salt concentrations over the Indian Ocean (Figure 2) show a similar spatial distribution to the [Na^+] measurements from the two INDOEX cruises (Figure 3), with higher concentrations south of the equator due to stronger winds.

5. Sea-Salt Aerosol Alkalinity and Sulfate Production

[24] Sea-salt aerosol alkalinity is consumed rapidly by uptake of SO_2 (g), H_2SO_4 (g), and HNO_3 (g). To describe this process in the model, we start by calculating the fluxes of the three acids to sea-salt aerosols in the MBL column by assuming that the alkalinity is present in excess. We then compare the sum of these fluxes to the local emission flux of alkalinity. If alkalinity is indeed in excess, then the rate of S(IV) + O_3 in sea-salt aerosols is calculated as the SO_2 flux. We assume that the excess alkalinity is eventually removed by uptake of carboxylic acids [*Mochida et al.*, 2003; *Legrand et al.*, 2004] or hydrochloric acid (HCl) or by deposition to the oceans; it is not transported outside of the MBL in the model. If alkalinity is not in excess, we assume that SO_2 (g), H_2SO_4 (g), and HNO_3 (g) compete for the available alkalinity on the basis of their relative fluxes. Aerosol neutralization by NH_3 is not significant above pH values of ~6 [*Jacob et al.*, 1986; *Shi et al.*, 1999] and so is not considered here for sea-salt aerosols.

[25] Uptake of SO_2 (g) by sea-salt aerosols is driven by the SO_3^{2-} + O_3 aqueous phase reaction with a rate constant $k = 1.5 \pm 0.6 \times 10^9$ mol L^{-1} s^{-1} [*Hoffmann and Calvert*, 1985]. For a pH = 8, a typical O_3 concentration of 30 ppb, and a Henry's law constant for O_3 of 1.1×10^{-2} mol L^{-1} atm^{-1} [*Seinfeld and Pandis*, 1998] we obtain a first-order loss rate constant for S(IV) in the aqueous phase $k_{chem} = k[O_3][SO_3^{2-}]/[S(IV)] = 4.4 \times 10^{-1}$ s^{-1}. This loss rate constant is sufficiently fast that the overall reaction rate is limited by SO_2 transfer from the gas to the aerosol phase [*Jacob*, 2000; *Liao et al.*, 2004]. Ozone, present at much higher concentrations than SO_2, is in excess. We express the SO_2 transfer rate constant (k_t) following the formulation of *Schwartz* [1986]:

$$k_t = \int_{r_0}^{r_0+\Delta r} \left(\frac{r}{D} + \frac{4}{v\alpha}\right)^{-1} 4\pi r^2 N(r) dr, \qquad (3)$$

integrated over each particle radius bin [r_0, $r_0 + \Delta r$]. Here $N(r)dr$ is the number concentration of sea-salt particles of radius [r, $r + dr$] derived from the *Monahan et al.* [1986] emission formulation and allowing for hygroscopic growth as a function of local relative humidity, $D = 0.2$ cm^2 s^{-1} is the gas phase molecular diffusion coefficient of SO_2 in air, $v = 3 \times 10^4$ cm s^{-1} is the mean molecular speed, and $\alpha = 0.11$ is the mass accommodation coefficient for SO_2 on liquid water surfaces [*Worsnop et al.*, 1989].

[26] Uptakes of H_2SO_4 (g) and HNO_3 (g) by sea-salt aerosols are similarly limited by transfer to the aerosol surface [*Abbatt and Waschewsky*, 1998; *Song and Carmichael*, 1999; *Guimbaud et al.*, 2002]. We estimate the uptake rate of H_2SO_4 (g) by aerosols from the production rate of H_2SO_4 (g) through (R1), partitioned between sea-salt and H_2SO_4-HNO_3-NH_3-H_2O aerosols on the basis of their locally computed relative surface areas in the model. For the latter we assume a lognormal size distribution with mean radius $\bar{r} = 0.082$ μm and geometric standard deviation of 2.0 to determine surface area. The sea-salt aerosol surface area is calculated by integrating the emission flux (particle m^{-2} s^{-1}) for each size bin [*Monahan et al.*, 1986]. The computation of HNO_3 (g) concentrations in the aerosol-oxidant GEOS-CHEM simulation of *Park et al.* [2004] is biased high because uptake by aerosols is considered only through the HNO_3-H_2SO_4-NH_3 system and does not include uptake by sea salt. To deal with this problem, we use the locally computed HNO_3 (g) deposition flux to the ocean in GEOS-CHEM as representing, in fact, uptake by sea-salt aerosols. The lifetime of HNO_3 (g) against deposition to the ocean surface (~1 day) is sufficiently long compared with uptake by sea-salt aerosols (~1 hour) that the latter will indeed dominate as long as the aerosols remain alkaline.

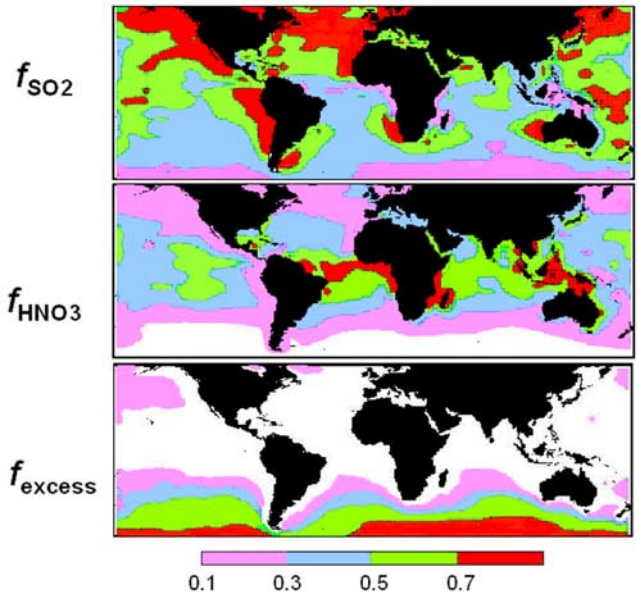

Figure 4. Fraction of emitted sea-salt alkalinity that is titrated by (top) the S(IV) + O_3 reaction (f_{SO2}) and by (middle) condensation of HNO_3 (g) (f_{HNO3}) in the GEOS-CHEM model simulation on an annual mean basis. (bottom) Mean fraction (f_{excess}) of total alkalinity remaining after titration by the S(IV) + O_3 reaction, HNO_3 (g), and H_2SO_4 (g).

[27] We find in this manner that sea-salt aerosol alkalinity is usually titrated by excess acidity, on a timescale of <1 hour following emission, for most oceanic conditions. Exceptions are remote oceanic regions with high sea-salt emissions, such as the Southern Ocean. Uptakes of SO_2 (g) and HNO_3 (g) are both important for titrating sea-salt aerosol alkalinity, their relative importance depending on region (Figure 4). Uptake of H_2SO_4 (g) is negligible in comparison because of low surface concentrations and competition with condensation on H_2SO_4-HNO_3-NH_3-H_2O aerosols. Titration by SO_2 is most important at extratropical northern latitudes where anthropogenic emissions (including ship emissions) are high. Titration by HNO_3 (g) is most important in the tropics where NO_x emissions from soils, biomass burning, and lightning dominate over SO_2 emissions.

6. Model Evaluation With INDOEX Measurements

[28] We ran two GEOS-CHEM simulations for the period of each cruise, one with S(IV) oxidation in sea-salt aerosols as described in section 5 and one without. The model was sampled as 24-hour averages along the track of each cruise. Since the model does not resolve the sulfate size distribution, the observed $\Delta^{17}O$ data for the coarse and fine size ranges were combined to give a bulk $\Delta^{17}O$ value for each sample ($\Delta^{17}O_{bulk} = \chi\Delta^{17}O_{fine} + (1 - \chi)\Delta^{17}O_{coarse}$, where χ is the fraction of total $nssSO_4^{2-}$ in the fine size range). The comparison between simulated and observed bulk $\Delta^{17}O$ is shown in Figure 5 for the pre-INDOEX 1997 (Figure 5, top) and 1998 INDOEX (Figure 5, bottom) cruises. $\Delta^{17}O$ values in the simulation with no sea-salt chemistry are always <1‰, while the simulation with sea-salt chemistry shows a similar range as the measurements (~0.5–3‰ for pre-INDOEX 1997 and ~0.5–2‰ for INDOEX 1998) and a similar latitudinal structure ($\Delta^{17}O$ > 1‰ only south of the equator). The latitudinal structure of $\Delta^{17}O$ in the model is driven by sea-salt emissions, as illustrated in Figure 2 by the strong gradient of sea-salt concentrations along the cruise tracks.

[29] For the pre-INDOEX 1997 cruise we ran two additional sensitivity simulations. In the first sensitivity simulation we investigated the effect of an additional biogenic alkalinity source in sea-salt aerosols by doubling the alkalinity flux (0.14 eq kg^{-1}) on the basis of the suggested 1–2.5 times enhancement of alkalinity indicated by calcium measurements from the western Pacific Ocean [*Sievering et al.*, 2004]. This results in a 50–100% increase in the amount of sulfate formed in sea-salt aerosols (3–38% of total sulfate along the cruise track, compared to 2–24% in the standard simulation), with an increase in $\Delta^{17}O$ sulfate values of 0.1–1.1‰ (Figure 6, top). This simulation reproduces the latitudinal trend in $\Delta^{17}O$ values; however, unlike the observations, all $\Delta^{17}O$ values are ≥1‰, and the maxi-

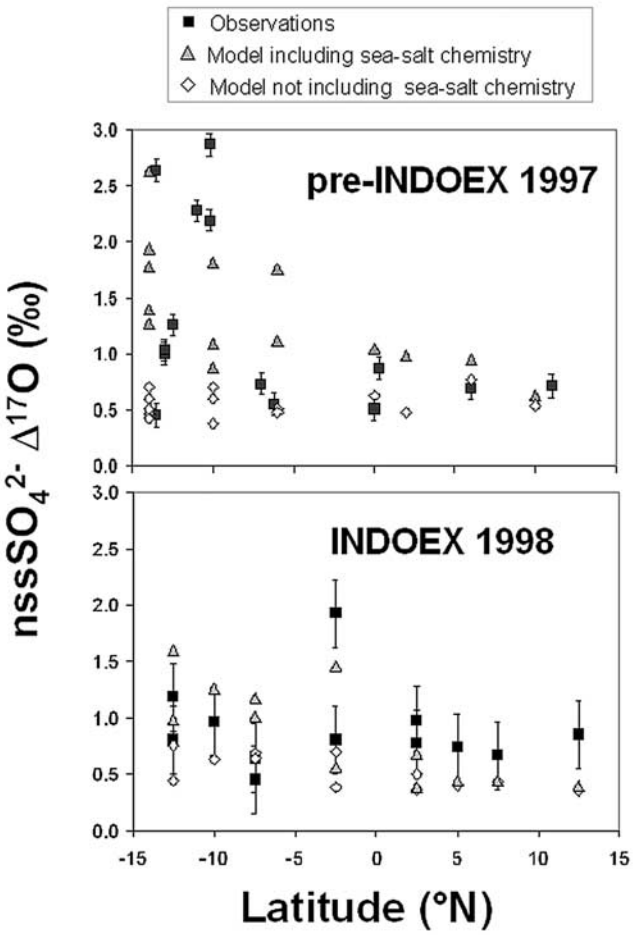

Figure 5. Bulk $nssSO_4^{2-}$ $\Delta^{17}O$ plotted as a function of latitude for the (top) 1997 pre-INDOEX and (bottom) 1998 INDOEX cruises. Observations (squares) are compared to model simulations including (triangles) and not including (diamonds) the production of sulfate in sea-salt aerosols.

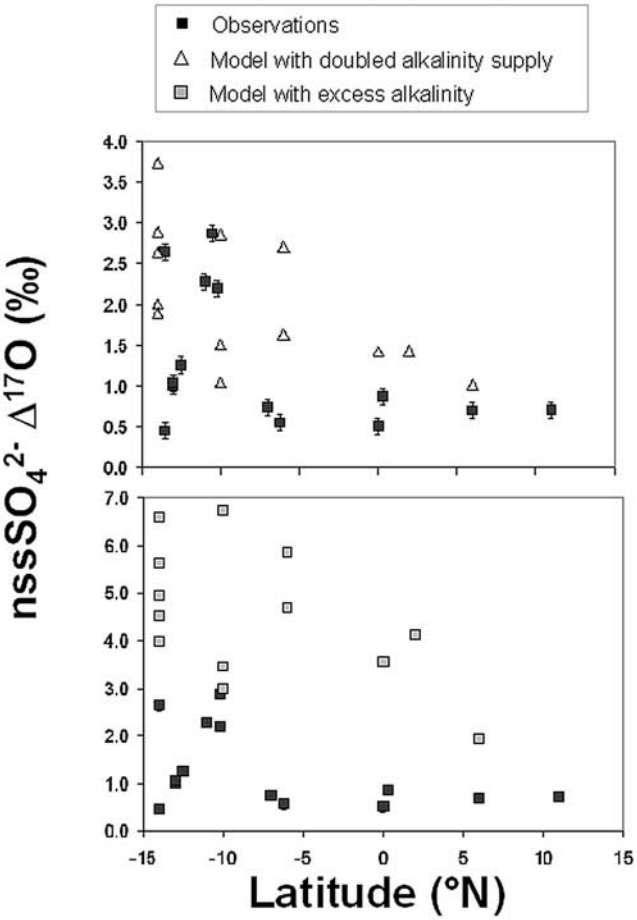

Figure 6. Bulk $nssSO_4^{2-}$ $\Delta^{17}O$ plotted as a function of latitude for the 1997 pre-INDOEX cruise. Observations (solid squares) are compared to two sensitivity model simulations. (top) First simulation, in which the sea-salt alkalinity flux is doubled to account for a possible additional biogenic alkalinity source (open triangles). (bottom) Second simulation, in which we assume continual regeneration of sea-salt alkalinity (shaded squares). The observations are the same as in Figure 5 (top), but the scales are different for each plot.

mum $\Delta^{17}O$ value overestimates the observations by 0.8‰. Chlorophyll images from Sea-viewing Wide Field-of-view Sensor (SeaWIFS) (available at http://seawifs.gsfc.nasa.gov/seawifs.html) indicate that oceanic productivity is relatively low in the Indian Ocean during January to March 1998 (data are not available for January 1997). The contribution of biogenic alkalinity and its effects on the sulfur budget will vary with oceanic productivity [*Sievering et al.*, 2004]. The impact of a biogenic alkalinity source would be better tested with sulfate $\Delta^{17}O$ measurements in a region of high oceanic productivity and high acid flux such as the North Atlantic.

[30] In the second sensitivity simulation we assumed that OH uptake by sea-salt aerosols always maintains an excess of alkalinity [*Laskin et al.*, 2003]. The $\Delta^{17}O$ values in this simulation greatly overestimate the measurements (Figure 6). We conclude that regeneration of alkalinity does not, in fact, take place, consistent with the observations of *Keene et al.* [2002].

7. Implications for the Sulfur Budget

[31] Table 2 presents the GEOS-CHEM global budgets for sulfate produced by different oxidation pathways. For a general discussion of the GEOS-CHEM global sulfate budget, including comparisons to other models, see *Park et al.* [2004] and *Martin et al.* [2004]. Sulfate formed by gas phase oxidation has the longest lifetime (6.1 days) because of a relatively high contribution from dry regions and high altitudes. The shortest lifetime (0.5 days) is for sulfate formed on coarse sea-salt aerosols. Wet processes account for 85% of deposition for total sulfate and dominate except for sulfate formed in coarse sea-salt aerosols. Sulfate formed on sea-salt aerosols accounts for 9% of global sulfate production but only 1% of the global sulfate burden. *Liao et al.* [2004] found a much larger contribution to the burden (13%) because they assumed, following *Laskin et al.* [2003], that reaction of OH with sea-salt aerosols would sustain alkalinity. As we have seen, this is not consistent with the oxygen isotope data.

[32] In our model, sulfate produced via S(IV) + O_3 in clouds is 4 times more abundant globally than sulfate produced by the same process in sea-salt aerosols. This is despite our assumption of a uniform cloud water pH of 4.5, greatly limiting the importance of the S(IV) + O_3 relative to the S(IV) + H_2O_2 pathway. The contribution from the S(IV) + O_3 in-cloud reaction is largely confined to the Northern Hemispheric winter when H_2O_2 is titrated [*Kleinman and Daum*, 1991; *Feichter et al.*, 1996], but there are large uncertainties with this result involving SO_2 oxidation on ice (in our model, in-cloud oxidation shuts down at temperatures below 258 K) and the competition from other non-photochemical oxidants [*Feichter et al.*, 1996; *Kasibhatla et al.*, 1997; *Leriche et al.*, 2003]. $\Delta^{17}O$ measurements of sulfate in that environment could effectively resolve these issues.

Table 2. GEOS-CHEM Global Budgets for Sulfate Produced by Different Oxidation Pathways

	Source, Tg S yr^{-1}	Dry Deposition[a]	Wet Deposition[a]	Lifetime, days	Burden, Tg S
Total sulfate	31.0	15%	85%	4.1	0.35
SO_2 + OH (gas phase)	8.2	15%	85%	6.1	0.14
S(IV) + H_2O_2 (in cloud)	15.7	7%	93%	4.0	0.17
S(IV) + O_3 (in cloud)	2.3	13%	87%	3.1	0.02
S(IV) + O_3 (fine sea salt)	0.4	8%	92%	1.7	0.002
S(IV) + O_3 (coarse sea salt)	2.3	62%	38%	0.5	0.003
Primary anthropogenic	2.0	20%	80%	3.7	0.02

[a]As percentages of total deposition, which balances production.

[33] Figure 7 shows the relative effect of sea-salt chemistry on simulated yearly mean SO_2 and sulfate concentrations in the MBL. Concentrations of SO_2 decrease by 10–30% over most of the oceans, up to a maximum of >70% over the Southern Ocean. Formation of sulfate in sea-salt aerosols could either increase total sulfate (by competing with SO_2 deposition) or decrease it (because of faster dry deposition leading to shorter sulfate lifetime). We find that sulfate concentrations increase slightly in much of the MBL, up to a maximum of 30% in the tropical South Pacific. In that region, rapid wet deposition (due to strong convection) makes the negative effect on sulfate concentrations relatively less important. Using a global model, *Gong and Barrie* [2003] previously examined the effect of sea-salt aerosols on the sulfur budget in the MBL due to condensation and coagulation processes and found decreases of 5–75% in sulfate concentrations in the MBL as a result of condensation of H_2SO_4 (g) followed by deposition. Our simulation does not account for this effect but indicates that it would be partially compensated by SO_2 oxidation in sea-salt aerosols, not taken into account by *Gong and Barrie* [2003].

[34] Figure 7 also shows the impact of sea-salt chemistry on simulated yearly mean H_2SO_4 (g) production rates by (R1) in the MBL. The decrease is usually <30 but >50% over the Southern Ocean. This would tend to decrease the potential for formation of new particles over the oceans. The effect tends to be greatest where sea-salt aerosol concentrations are highest, and these are not regions propitious for formation of new particles in any case. Nevertheless, the widespread nature of the effect (10–30% over most of the oceans) suggests that it could be of some importance for model simulations of aerosol nucleation.

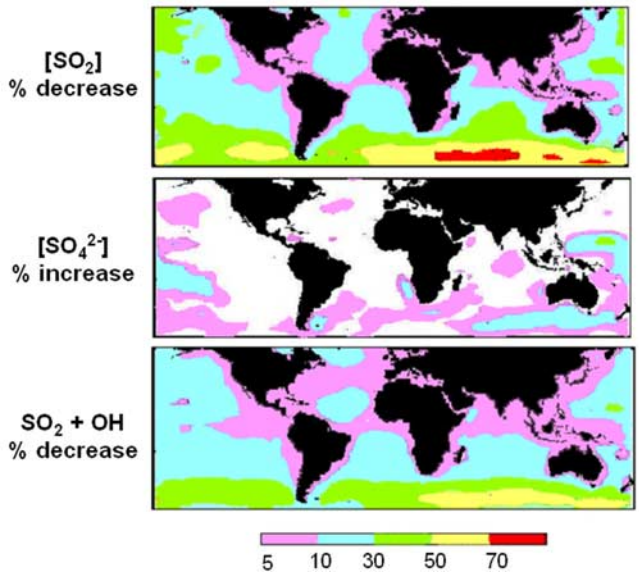

Figure 7. Effect of sea-salt chemistry on simulated yearly mean SO_2 concentrations, sulfate concentrations, and the rate of gas phase sulfate formation (SO_2 + OH) in the marine boundary layer at 0–100 m altitude.

8. Conclusions

[35] Measurement of the mass-independent composition of the oxygen isotopes ($\Delta^{17}O \neq 0$) of atmospheric sulfate aerosol provides quantitative insight into the oxidation pathways responsible for sulfate formation. A positive $\Delta^{17}O$ implies aqueous phase formation involving oxidation of S(IV) by H_2O_2 or O_3. A $\Delta^{17}O > 1‰$ specifically implies aqueous phase oxidation by O_3 [*Savarino et al.*, 2000]. The latter reaction can proceed at a significant rate only at relatively high pH (>6). Measurements presented here from two INDOEX ship cruises over the Indian Ocean show frequent occurrences of $\Delta^{17}O > 1‰$ in regions of high sea-salt concentrations but not elsewhere. This provides evidence for sulfate formation in alkaline sea-salt aerosols by the S(IV) + O_3 pathway.

[36] We used the GEOS-CHEM global chemical transport model to interpret the $\Delta^{17}O$ observations and to place them in a global context. We showed that the extent of sulfate formation in sea-salt aerosols is usually limited by the alkalinity flux associated with sea-salt aerosol emission and by competition for this alkalinity supply from HNO_3 (g). Once the alkalinity of the sea-salt aerosols has been titrated, the pH drops abruptly, and sulfate formation shuts off. In the extratropical Southern Hemisphere where the sea-salt alkalinity flux often exceeds the availability of strong acids, sulfate formation in sea-salt aerosols is limited by the gas-to-particle transfer rate of SO_2.

[37] We find that a model simulation including S(IV) + O_3 oxidation in alkaline sea-salt aerosols, and accounting for acid titration of sea-salt alkalinity, can reproduce the range and latitudinal structure of the observed $\Delta^{17}O$ sulfate values from the two INDOEX ship cruises. The latitudinal structure of $\Delta^{17}O$ in the model is driven by sea-salt emissions. A sensitivity simulation with a doubled alkalinity flux, to account for a possible biogenic alkalinity ($CaCO_3$) source, produces similar results in terms of the latitudinal trend in the $\Delta^{17}O$ observations, with a 0.8‰ overestimate of the maximum $\Delta^{17}O$ observation. The potential impact of a biogenic alkalinity source on the sulfur budget in the MBL could be better tested with sulfate $\Delta^{17}O$ measurements in a region of high oceanic productivity and high acid flux such as the North Atlantic. Another sensitivity simulation not accounting for titration of alkalinity (i.e., assuming that alkalinity always remains in excess) greatly overestimates (by 3.8‰) the $\Delta^{17}O$ observations. This argues against the hypothesis that sea-salt alkalinity is regenerated in the atmosphere by the NaCl + OH reaction [*Laskin et al.*, 2003].

[38] We applied the GEOS-CHEM model with the above constraints to quantify the impact on the atmospheric sulfur budget of sulfate formation in sea-salt aerosols. Sulfate formed in sea-salt aerosols has a short lifetime (0.5–1.7 days) compared to sulfate formed in the gas phase or in clouds (3.1–6.1 days) and accounts for 9 and 1% of total global sulfate production and burden, respectively. This sea-salt chemistry decreases SO_2 concentrations in the MBL by typically 10–30% but by >70% over the Southern Ocean. It increases sulfate concentrations by up to 30%. This chemical enhancement of sulfate in the MBL offsets, at least in part, the depletion due to condensation of H_2SO_4 (g) onto sea-salt particles followed by dry deposition [*Gong et al.*, 2002]. Sulfate formation in sea-salt aerosols also leads to reductions in the rate of gas phase H_2SO_4 formation by 10–30% over

much of the world's oceans. This would tend to decrease the potential formation of new particles over the oceans and hence any possible thermostat involving production of CCN from temperature-dependent DMS emissions.

[39] $\Delta^{17}O$ measurements of sulfate aerosols collected at various continental sites also show values >1‰ [*Lee et al.*, 2001; *Lee and Thiemens*, 2001; *Bao and Reheis*, 2003], indicating potential sources of continental alkalinity. Laboratory experiments have observed sulfate formation on dust when exposed to SO_2 and O_3 [*Ullerstam et al.*, 2002], perhaps at least partially explaining these large continental $\Delta^{17}O$ values. Ice core sulfate $\Delta^{17}O$ measurements are available from Greenland and Antarctica extending through the last interglacial period and show values in the range of 0.2–4.8‰, varying with climate on the glacial-interglacial timescale [*Alexander et al.*, 2002, 2004]. Interpretation of these ice core data with a global 3-D paleoclimate model could provide important new information on trends in sulfur and oxidant budgets over Earth's history.

[40] **Acknowledgments.** Financial support for this project was provided by a NOAA CGC postdoctoral fellowship to B. Alexander and by the NSF Atmospheric Chemistry Program. The GEOS-CHEM model is managed at Harvard University with support from the NASA Atmospheric Chemistry and Modeling Analysis Program. B. Alexander is a Daly postdoctoral fellow in the Department of Earth and Planetary Sciences, Harvard University.

References

Abbatt, J. P. D., and G. C. G. Waschewsky (1998), Heterogeneous interactions of OHBr, HNO_3, O_3, and NO_2 with deliquescent NaCl aerosols at room temperature, *J. Phys. Chem. A*, *102*, 3719–3725.

Alexander, B., J. Savarino, N. I. Barkov, R. J. Delmas, and M. H. Thiemens (2002), Climate driven changes in the oxidation pathways of atmospheric sulfur, *Geophys. Res. Lett.*, *29*(14), 1685, doi:10.1029/2002GL014879.

Alexander, B., J. Savarino, K. J. Kreutz, and M. H. Thiemens (2004), Impact of preindustrial biomass-burning emissions on the oxidation pathways of tropospheric sulfur and nitrogen, *J. Geophys. Res.*, *109*, D08303, doi:10.1029/2003JD004218.

Andronache, C., W. L. Chameides, D. D. Davis, B. E. Anderson, R. F. Pueschel, A. R. Bandy, D. C. Thornton, R. W. Talbot, P. Kasibhatla, and C. S. Kiang (1997), Gas-to-particle conversion of tropospheric sulfur as estimated from observations in the western North Pacific during PEM-West B, *J. Geophys. Res.*, *102*(D23), 28,511–28,538.

Bao, H., and M. C. Reheis (2003), Multiple oxygen and sulfur isotopic analysis on water-soluble sulfate in bulk atmospheric deposition from the southwestern United States, *J. Geophys. Res.*, *108*(D14), 4430, doi:10.1029/2002JD003022.

Barth, M. C., P. J. Rasch, and J. T. Kiehl (2000), Sulfur chemistry in the National Center for Atmospheric Research Community Climate Model: Description, evaluation, features, and sensitivity to aqueous chemistry, *J. Geophys. Res.*, *105*(D1), 1387–1415.

Bhattacharya, S. K., and M. H. Thiemens (1989), New evidence for symmetry dependent isotope effects: O + CO reaction, *Z. Naturforsch. A*, *44*, 435–444.

Brenninkmeijer, C. A. M., C. Janssen, J. Kaiser, T. Rockmann, T. S. Rhee, and S. S. Assonov (2003), Isotope effects in the chemistry of atmospheric trace compounds, *Chem. Rev.*, *103*(12), 5125–5161.

Calhoun, J. A., T. S. Bates, and R. J. Charlson (1991), Sulfur isotope measurements of submicrometer sulfate aerosol particles over the Pacific Ocean, *Geophys. Res. Lett.*, *18*(10), 1877–1880.

Calvert, J. G., A. Lazarus, G. L. Kok, B. G. Heikes, J. G. Walega, J. Lind, and C. A. Cantrell (1985), Chemical mechanisms of acid generation in the troposphere, *Nature*, *317*, 27–35.

Chameides, W. L. (1984), The photochemistry of remote marine stratiform cloud, *J. Geophys. Res.*, *89*(D3), 4739–4755.

Chameides, W. L., and A. W. Stelson (1992), Aqueous-phase chemical processes in deliquescent sea-salt aerosols: A mechanism that couples the atmospheric cycles of S and sea salt, *J. Geophys. Res.*, *97*(D18), 20,565–20,580.

Charlson, R. J., J. E. Lovelock, M. O. Andreae, and S. G. Warren (1987), Oceanic phytoplankton, atmospheric sulphur, cloud albedo and climate, *Nature*, *326*, 655–661.

Chin, M., D. J. Jacob, G. M. Gardner, M. S. Foreman-Fowler, and P. A. Spiro (1996), A global three-dimensional model of tropospheric sulfate, *J. Geophys. Res.*, *101*(D13), 18,667–18,690.

Chin, M., R. B. Rood, S.-J. Lin, F.-F. Muller, and A. M. Thompson (2000), Atmospheric sulfur cycle simulated in the global model GOCART: Model description and global properties, *J. Geophys. Res.*, *105*(D20), 24,671–24,687.

Chin, M., P. Ginoux, S. Kinne, O. Torres, B. N. Holben, B. N. Duncan, R. V. Martin, J. A. Logan, A. Higurashi, and T. Nakajima (2002), Tropospheric aerosol optical thickness from the GOCART model and comparisons with satellite and sun photometer measurements, *J. Atmos. Sci.*, *59*, 461–483.

Corbett, J. J., P. S. Fischbeck, and S. N. Pandis (1999), Global nitrogen and sulfur inventories for oceangoing ships, *J. Geophys. Res.*, *104*(D3), 3457–3470.

Davies, J. A., and R. A. Cox (1998), Kinetics of heterogeneous reaction of HNO_3 with NaCl: Effect of water vapor, *J. Phys. Chem. A*, *102*, 7631–7642.

Dentener, F., J. Williams, and S. Metzger (2002), Aqueous phase reaction of HNO_4: The impact on tropospheric chemistry, *J. Atmos. Chem.*, *41*, 109–134.

Dubey, M. K., R. Mohrschladt, N. M. Donahue, and J. G. Anderson (1997), Isotope-specific kinetics of hydroxyl radical (OH) with water (H_2O): Testing models of reactivity and atmospheric fractionation, *J. Phys. Chem. A*, *101*, 1494–1500.

Farquhar, J., J. Savarino, T. L. Jackson, and M. H. Thiemens (2000), Evidence of atmospheric sulfur in the Martian regolith from sulphur isotopes in meteorites, *Nature*, *404*, 50–52.

Feichter, J., E. Kjellstrom, H. Rodhe, F. Dentener, J. Lelieveld, and G.-J. Roelofs (1996), Simulation of the tropospheric sulfur cycle in a global climate model, *Atmos. Environ.*, *30*, 1693–1707.

Feingold, G., G. J. Frost, and A. R. Ravishankara (2002), Role of NO_3 in sulfate production in the wintertime northern latitudes, *J. Geophys. Res.*, *107*(D22), 4640, doi:10.1029/2002JD002288.

Gerber, H. E. (1985), Relative-humidity parameterization of the Navy aerosol model (NAM), *NRL Rep. 8956*, Natl. Res. Lab., Washington, D. C.

Gong, S. L., and L. A. Barrie (2003), Simulating the impact of sea salt on global nss sulphate aerosols, *J. Geophys. Res.*, *108*(D16), 4516, doi:10.1029/2002JD003181.

Gong, S. L., L. A. Barrie, and M. Lazare (2002), Canadian Aerosol Module (CAM): A size-segregated simulation of atmospheric aerosol processes for climate and air quality models—2. Global sea-salt aerosol and its budgets, *J. Geophys. Res.*, *107*(D24), 4779, doi:10.1029/2001JD002004.

Grini, A., G. Myhre, J. Sundet, and I. S. A. Isaksen (2002), Modeling the annual cycle of sea salt in the global 3D model Oslo CTM2: Concentrations, fluxes, and radiative impact, *J. Clim.*, *15*, 1717–1730.

Guimbaud, C., F. Arens, L. Gutzwiller, H. W. Gaggeler, and M. Ammann (2002), Uptake of HNO_3 to deliquescent sea-salt particles: A study using the short-lived radioactive isotope tracer ^{13}N, *Atmos. Chem. Phys.*, *2*, 249–257.

Gurciullo, C., B. Lerner, H. Sievering, and S. N. Pandis (1999), Heterogeneous sulfate production in the remote marine environment: Cloud processing and sea-salt particle contributions, *J. Geophys. Res.*, *104*(D17), 21,719–21,731.

Hoffmann, M. R., and J. G. Calvert (1985), Chemical transformation modules for Eulerian acid deposition models, vol. 2, The aqueous-phase chemistry, *Rep. EPA/600/3-85/017*, U.S. Environ. Prot. Agency, Research Triangle Park, N. C.

Holt, B. C., R. Kumar, and P. T. Cunningham (1981), Oxygen-18 study of the aqueous-phase oxidation of sulfur dioxide, *Atmos. Environ.*, *15*, 557–566.

Intergovernmental Panel on Climate Change (2001), Radiative forcing and climate change, in *Climate Change 2001: The Scientific Basis—Contribution of Working Group I to the Third Assessment Report of the Intergovernmental Panel on Climate Change*, edited by V. Ramaswamy, p. 8, Cambridge Univ. Press, New York.

Jacob, D. J. (2000), Heterogeneous chemistry and tropospheric ozone, *Atmos. Environ.*, *34*, 2131–2159.

Jacob, D. J., and M. R. Hoffmann (1983), A dynamic model for the production of H^+, NO_3^-, and SO_4^{2-} in urban fog, *J. Geophys. Res.*, *88*(C11), 6611–6621.

Jacob, D. J., J. M. Waldman, J. W. Munger, and M. R. Hoffmann (1986), The H_2SO_4-HNO_3-NH_3 system at high humidities and in fogs: 2. Comparison of field data with thermodynamic calculations, *J. Geophys. Res.*, *91*(D1), 1089–1096.

Janssen, C., J. Guenther, and D. Krankowsky (1999), Relative formation rates of $^{50}O_3$ and $^{52}O_3$ in ^{16}O-^{18}O mixtures, *J. Chem. Phys.*, *111*(16), 7179–7182.

Kasibhatla, P., W. L. Chameides, and J. St. John (1997), A three-dimensional global model investigation of seasonal variations in the atmo-

spheric burden of anthropogenic sulfate aerosols, *J. Geophys. Res.*, *102*(D3), 3737–3759.
Katoshevski, D., A. Nenes, and J. H. Seinfeld (1999), A study of processes that govern the maintenance of aerosols in the marine boundary layer, *J. Aerosol Sci.*, *30*(4), 503–532.
Keene, W. C., and A. P. Pszenny (2004), Comment on "Reactions at interfaces as a source of sulfate formation in sea-salt particles" (I), *Science*, *303*, 628.
Keene, W. C., A. A. P. Pszenny, J. R. Maben, and R. Sander (2002), Variation of marine aerosol acidity with particle size, *Geophys. Res. Lett.*, *29*(7), 1101, doi:10.1029/2001GL013881.
Kleinman, L. I., and P. H. Daum (1991), Oxidant limitation to the formation of sulfuric acid near a sulfur dioxide source region, *Atmos. Environ. Part A*, *25*, 2023–2028.
Koch, D., D. Jacob, I. Tegan, D. Rind, and M. Chin (1999), Tropospheric sulfur simulation and sulfate direct radiative forcing in the Goddard Institute for Space Studies general circulation model, *J. Geophys. Res.*, *104*(D19), 23,799–23,822.
Kulshrestha, U. C., M. Jain, T. K. Mandal, P. K. Gupta, A. K. Sarkar, and D. C. Parashar (1999), Measurements of acid rain over Indian Ocean and surface measurements of atmospheric aerosols at New Delhi during INDOEX pre-campaigns, *Curr. Sci.*, *76*(7), 968–972.
Kumala, M., L. Pirjoia, and J. M. Makela (2000), Stable sulphate clusters as a source of new atmospheric particles, *Nature*, *404*, 66–69.
Laskin, A., D. J. Gaspar, W. Want, S. W. Hunt, J. P. Cowin, S. D. Colson, and B. J. Finlayson-Pitts (2003), Reactions at interfaces as a source of sulfate formation in sea-salt particles, *Science*, *301*, 340–344.
Lee, C. C. W., and M. H. Thiemens (2001), The $\delta^{17}O$ and $\delta^{18}O$ measurements of atmospheric sulfate from a coastal and high alpine region: A mass-independent anomaly, *J. Geophys. Res.*, *105*(D15), 17,359–17,373.
Lee, C. C. W., J. Savarino, and M. H. Thiemens (2001), Mass independent oxygen isotopic composition of atmospheric sulfate: Origin and implications for the present and past atmospheres of Earth and Mars, *Geophys. Res. Lett.*, *28*(9), 1783–1786.
Lee, C. C. W., J. Savarino, H. Cachier, and M. H. Thiemens (2002), Sulfur (^{32}S, ^{33}S, ^{34}S, ^{36}S) and oxygen (^{16}O, ^{17}O, ^{18}O) isotopic ratios of primary sulfate produced from combustion processes, *Tellus, Ser. B*, *54*, 193–200.
Lee, Y. N., and S. E. Schwartz (1983), Kinetics of oxidation of aqueous sulfur (IV) by nitrogen dioxide, in *Precipitation Scavenging, Dry Deposition, and Resuspension, Proceedings of the Fourth International Conference, Santa Monica, California, 29 November–3 December 1982*, vol. 1, edited by H. R. Pruppacher and W. G. N. Slinn, pp. 453–470, Elsevier, New York.
Legrand, M., S. Preunkert, and B. Jourdain (2004), Year-round records of gas and particulate formic and acetic acids in the boundary layer at Dumont d'Urville, coastal Antarctica, *J. Geophys. Res.*, *109*, D06313, doi:10.1029/2003JD003786.
Leriche, M., L. Deguillaume, and N. Chaumerliac (2003), Modeling study of strong acids formation and partitioning in a polluted cloud during wintertime, *J. Geophys. Res.*, *108*(D14), 4433, doi:10.1029/2002JD002950.
Liao, H., P. J. Adams, S. H. Chung, J. H. Seinfeld, L. J. Mickley, and D. J. Jacob (2003), Interactions between tropospheric chemistry and aerosols in a unified general circulation model, *J. Geophys. Res.*, *108*(D1), 4001, doi:10.1029/2001JD001260.
Liao, H., J. H. Seinfeld, P. J. Adams, and L. J. Mickley (2004), Global radiative forcing of tropospheric ozone and aerosols in a unified general circulation model, *J. Geophys. Res.*, *109*, D16207, doi:10.1029/2003JD004456.
Liu, H., D. J. Jacob, I. Bey, and R. M. Yantosca (2001), Constraints from ^{210}Pb and ^{7}Be on wet deposition and transport in a global three-dimensional chemical tracer model driven by assimilated meterological fields, *J. Geophys. Res.*, *106*(D11), 12,109–12,128.
Lyons, J. R. (2001), Transfer of mass-independent fractionation on ozone to other oxygen-containing molecules in the atmosphere, *Geophys. Res. Lett.*, *28*(17), 3231–3234.
Martin, S. T., H.-M. Hung, R. J. Park, D. J. Jacob, R. J. D. Spurr, K. V. Chance, and M. Chin (2004), Effects of the physical state of tropospheric ammonium-sulfate-nitrate particles on global aerosol direct radiative forcing, *Atmos. Chem. Phys.*, *4*, 183–214.
Matsuhisa, Y., J. R. Goldsmith, and R. N. Clayton (1978), Mechanisms of hydrothermal crystallization of quartz at 250C and 15 kbar, *Geochim. Cosmochim. Acta*, *42*, 173–182.
Mauersberger, K., B. Erbacher, D. Krankowsky, J. Gunther, and R. Nickel (1999), Ozone isotope enrichment: Isotopomer-specific rate coefficients, *Science*, *283*, 370–372.
McArdle, J. V., and M. R. Hoffmann (1983), Kinetics and mechanism of the oxidation of aquated sulfur dioxide by hydrogen peroxide at low pH, *J. Phys. Chem.*, *87*, 5425–5429.
Mochida, M., N. Umemoto, K. Kawamura, and M. Uematsu (2003), Bimodal size distribution of C2-C4 dicarboxylic acids in the marine aerosols, *Geophys. Res. Lett.*, *30*(13), 1672, doi:10.1029/2003GL017451.
Monahan, E. C., D. E. Spiel, and K. L. Davidson (1986), A model of marine aerosol generation via whitecaps and wave disruption, in *Oceanic Whitecaps and Their Role in Air-Sea Exchange Processes*, edited by E. C. Monahan and G. M. Niocaill, pp. 167–174, Springer, New York.
Morton, J., J. Barnes, B. Schueler, and K. Mauersberger (1990), Laboratory studies of heavy ozone, *J. Geophys. Res.*, *95*(D1), 901–907.
Park, R. J., D. J. Jacob, B. D. Field, R. M. Yantosca, and M. Chin (2004), Natural and transboundary pollution influences on sulfate-nitrate-ammonium aerosols in the United States: Implications for policy, *J. Geophys. Res.*, *109*, D15204, doi:10.1029/2003JD004473.
Ramanathan, V., et al. (2001), Indian Ocean Experiment: An integrated analysis of the climate forcing and effects of the great Indo-Asian haze, *J. Geophys. Res.*, *106*(22), 28,371–28,398.
Sander, R., P. J. Crutzen, and R. von Glasow (2004), Comment on "Reactions at Interfaces as a Source of Sulfate Formation in Sea-Salt Particles" (II), *Science*, *303*, 628.
Savarino, J., and M. H. Thiemens (1999), Analytical procedure to determine both $\delta^{18}O$ and $\delta^{17}O$ of H_2O_2 in natural water and first measurements, *Atmos. Environ.*, *33*, 3683–3690.
Savarino, J., C. C. W. Lee, and M. H. Thiemens (2000), Laboratory oxygen isotopic study of sulfur (IV) oxidation: Origin of the mass-independent isotopic anomaly in atmospheric sulfates and sulfate mineral deposits on Earth, *J. Geophys. Res.*, *105*(D23), 29,079–29,088.
Savarino, J., B. Alexander, V. Darmohusodo, and M. H. Thiemens (2001), Sulfur and oxygen isotope analysis of sulfate at micromole levels using a pyrolysis technique in a continuous flow system, *Anal. Chem.*, *73*, 4457–4462.
Schwartz, S. E. (1986), Mass-transport considerations pertinent to aqueous-phase reactions of gases in liquid-water clouds, in *Chemistry of Multiphase Atmospheric Systems*, edited by W. Jaeschke, pp. 415–471, Springer, New York.
Schwartz, S. E. (1987), Aqueous-phase reactions in clouds, in *The Chemistry of Acid Rain: Sources and Atmospheric Processes*, edited by R. W. Johnson and G. E. Gordon, pp. 93–108, Am. Chem. Soc., Washington, D. C.
Seinfeld, J. H., and S. N. Pandis (1998), Chemistry of the aqueous phase, in *Atmospheric Chemistry and Physics: From Air Pollution to Climate Change*, pp. 337–407, Wiley-Interscience, Hoboken, N. J.
Shaw, G. E. (1983), Bio-controlled thermostasis involving the sulfur cycle, *Clim. Change*, *5*(3), 297–303.
Shi, Q., P. Davidovits, J. T. Jayne, D. R. Worsnop, and C. E. Kolb (1999), Uptake of gas-phase ammonia.1. Uptake by aqueous surfaces as a function of pH, *J. Phys. Chem. A*, *103*, 8812–8823.
Sievering, H., J. Boatman, J. Galloway, W. Keene, Y. Kim, M. Lauria, and J. Ray (1991), Heterogeneous sulfur conversion in sea salt aerosol particles: The role of aerosol water content and size distribution, *Atmos. Environ. Part A*, *25*, 1479–1487.
Sievering, H., J. Cainey, M. Harvey, J. McGregor, and S. Nichol (2004), Aerosol non-sea-salt sulfate in the remote marine boundary layer under clear-sky and normal cloudiness conditions: Ocean-derived biogenic alkalinity enhances sea-salt sulfate production by ozone oxidation, *J. Geophys. Res.*, *109*, D19317, doi:10.1029/2003JD004315.
Song, C. H., and G. R. Carmichael (1999), The aging process of naturally emitted aerosol (sea-salt and mineral aerosol) during long range transport, *Atmos. Environ.*, *33*, 2203–2218.
Song, C. H., and G. R. Carmichael (2001), A three-dimensional modeling investigation of the evolution processes of dust and sea-salt particles in east Asia, *J. Geophys. Res.*, *106*(D16), 18,131–18,154.
Stockwell, W. R., and J. G. Calvert (1983), The mechanism of the HO-SO_2 reaction, *Atmos. Environ.*, *17*, 2231–2235.
Takemura, T., H. Okamoto, Y. Maruyama, A. Numaguti, A. Higurashi, and T. Nakajima (2000), Global three-dimensional simulation of aerosol optical thickness distribution of various origins, *J. Geophys. Res.*, *105*(D14), 17,853–17,873.
Tegen, I., P. Hollrig, M. Chin, I. Fung, D. Jacob, and J. Penner (1997), Contribution of different aerosol species to the global aerosol extinction optical thickness: Estimates from model results, *J. Geophys. Res.*, *102*(D20), 23,895–23,915.
Ten Brink, H. M. (1998), Reactive uptake of HNO_3 and H_2SO_4 in sea-salt (NaCl) particles, *J. Aerosol Sci.*, *29*(1/2), 57–64.
Thiemens, M. H. (1999), Mass-independent isotope effects in planetary atmospheres and the early solar system, *Science*, *283*, 341–345.
Thiemens, M. H., and T. Jackson (1990), Pressure dependency for heavy isotope enhancement in ozone formation, *Geophys. Res. Lett.*, *17*(6), 717–719.

Tie, X., G. Brasseur, L. Emmons, L. Horowitz, and D. Kinnison (2001), Effects of aerosols on tropospheric oxidants: A global model study, *J. Geophys. Res.*, *106*(D19), 22,931–22,964.

Ullerstam, M., R. Vogt, S. Langer, and E. Ljungstrom (2002), The kinetics and mechanism of SO_2 oxidation by O_3 on mineral dust, *Phys. Chem. Chem. Phys.*, *4*, 4694–4699.

Vogt, R., P. J. Crutzen, and R. Sander (1996), A mechanism for halogen release from sea-salt aerosol in the marine boundary layer, *Nature*, *383*, 327–330.

von Glasow, R., and P. J. Crutzen (2004), Model study of multiphase DMS oxidation with a focus on halogens, *Atmos. Chem. Phys.*, *4*, 589–608.

von Glasow, R., R. Sander, A. Bott, and P. J. Crutzen (2002), Modeling halogen chemistry in the marine boundary layer: 2. Interactions with sulfur and the cloud-covered MBL, *J. Geophys. Res.*, *107*(D17), 4323, doi:10.1029/2001JD000943.

Wang, Y. H., D. J. Jacob, and J. A. Logan (1998), Global simulation of tropospheric O_3-NO_x-hydrocarbon chemistry: 1. Model formulation, *J. Geophys. Res.*, *103*(D9), 10,713–10,725.

Warneck, P. (1999), The relative importance of various pathways for the oxidation of sulfur dioxide and nitrogen dioxide in sunlit continental fair weather clouds, *Phys. Chem. Chem. Phys.*, *1*, 5471–5483.

Weber, R. J., G. Chen, D. D. Davis, R. L. Mauldin III, D. J. Tanner, F. L. Eisele, A. D. Clarke, D. C. Thornton, and A. R. Bandy (2001), Measurements of enhanced H_2SO_4 and 3–4 nm particles near a frontal cloud during the First Aerosol Characterization Experiment (ACE 1), *J. Geophys. Res.*, *106*(D20), 24,107–24,117.

Wesely, M. L. (1989), Parameterization of surface resistances to gaseous dry deposition in regional-scale numerical-models, *Atmos. Environ.*, *23*, 1293–1304.

Worsnop, D. R., M. S. Zahniser, C. E. Colb, J. A. Gardner, L. R. Watson, J. M. van Doren, J. T. Jayne, and P. Davidovits (1989), The temperature dependence of mass accommodation of SO_2 and H_2O_2 on aqueous surfaces, *J. Phys. Chem.*, *93*, 1159–1172.

Zhang, L., S. Gong, J. Padro, and L. Barrie (2001), A size-segregated particle dry deposition scheme for an atmospheric aerosol module, *Atmos. Environ.*, *35*, 549–560.

B. Alexander, Department of Atmospheric Sciences, University of Washington, Box 351640, Seattle, WA 98195, USA. (beckya@u.washington.edu)

D. J. Jacob, R. J. Park, and R. M. Yantosca, Department of Earth and Planetary Sciences, Harvard University, Cambridge, MA 02138, USA.

C. C. W. Lee, URS Corporation, 2020 East First Street, Suite 400, Santa Ana, CA 92705, USA.

Q. B. Li, Jet Propulsion Laboratory, 4800 Oak Grove Drive, M/S 183-501, Pasadena, CA 91109, USA.

J. Savarino, Laboratoire de Glaciologie et Géophysique de l'Environnement/CNRS, 54, Rue Moliere BP96, St. Martin d'Hères F-38402, France.

M. H. Thiemens, Department of Chemistry and Biochemistry, University of California, San Diego, 9500 Gilman Drive, La Jolla, CA 92093-0356, USA.